Proceedings of the Thirty-fifth (2025) International Ocean and Polar Engineering Conference **www.isope.org**
Seoul/Goyang, Korea, June 1-6, 2025

ISBN 978-1-880653-74-6; ISSN 1098-6189

Experimental and Numerical Modeling of Flexible Synthetic Mooring Lines for Floating Structures

Oriol Colomés, Juan Tang, Somansundar Sakthivel, Shagun Agarwal, Kevin Jonathan and Sergio Sanchez Gómez
Faculty of Civil Engineering and Geosciences, Delft University of Technology, The Netherlands

ABSTRACT

The expansion of floating offshore renewable energy demands reliable mooring solutions. Synthetic mooring ropes offer cost savings and performance benefits but exhibit complex, nonlinear, and frequency-dependent behavior. This study investigates their mechanical response through experimental testing, characterizing quasi-static and dynamic properties. The results inform a viscoelastic material model that captures nonlinear stiffness and dynamic response under marine loading. Based on Schapery's formulation, this model can be integrated into a Finite Element framework to simulate real-world conditions, improving predictive capabilities for synthetic mooring lines in offshore applications.

KEY WORDS: Floating offshore renewable energy; synthetic mooring ropes; nonlinear dynamic properties; viscoelastic material model; Finite Element modelling; offshore energy applications.

INTRODUCTION

The global push for sustainable energy has accelerated the development of floating offshore renewable energy systems such as wind turbines, offshore photovoltaics, and wave energy converters. These systems demand reliable and cost-effective mooring solutions to ensure their stability and longevity in dynamic and extreme marine environments. Synthetic mooring lines are a promising alternative to traditional steel cables due to their lightweight, flexibility, and reduced installation costs, making them particularly suited for floating renewable energy platforms (Bain et al. 2020; Chevillotte et al. 2020; Davies et al. 2011).

Mooring systems are critical for anchoring floating structures. Traditional steel cables, though strong, are prone to corrosion and lack flexibility. At the same time, synthetic ropes, made from materials like polyester and High Modulus Polyethylene (HMPE), offer superior fatigue resistance and adaptability to marine conditions (S.D. Weller et al. 2015; Sam Weller et al. 2014). However, modeling synthetic lines is challenging due to their nonlinear stiffness, frequency-dependent dynamics, and time-dependent behaviors such as creep and hysteresis, which impact long-term performance (Huang et al. 2015; Lian et al. 2018).

While experimental studies have provided insights into the mechanical properties of synthetic ropes, numerical models often struggle to replicate these behaviors under real-world conditions accurately (Chailleux and Davies 2005; Nguyen and Thiagarajan 2022). This paper addresses these gaps by integrating experimental findings with numerical modeling to predict synthetic mooring line performance under operational scenarios.

The objectives of this study are twofold: (1) to experimentally evaluate the mechanical properties of synthetic mooring lines, including quasi-static and dynamic characteristics; and (2) to develop a viscoelastic material model capturing their nonlinear and frequency-dependent behaviors. The resulting viscoelastic model can later be implemented in a finite element model to simulate mooring line dynamics in real-world loading conditions. This last step is considered out of the scope of the current work and will be contemplated in a follow-up study.

The paper is structured as follows: Section 2 outlines the physical experiments, including materials, setup, testing procedures and experimental results. Section 3 introduces the viscoelastic material model, detailing the theoretical stress-strain relation and parameter fitting that match the experimental results. In Section 4 we conclude the study with a summary of key findings and prospects for future research.

PHYSICAL EXPERIMENTS

Methodology

Materials and Setup

The experimental setup employed a high-precision jacking machine to apply and maintain tension accurately, allowing for a thorough evaluation polyester rope types. This study examines Kapa Polyester Plus ropes made from high-tenacity yarns with a braided core and a protective polyester jacket, which enhances ultraviolet (UV), abrasion, and particle resistance. The 52 mm diameter rope has a Minimum Breaking Load (MBL) of 104 tonnes and a Minimum Breaking Force (MBF) of 1021 kN. The study uses a hydraulic jack with an input pressure of 280 bar, a stroke length of 2000 mm, a maximum force capacity of 400 kN, and a shaft diameter of 110 mm. Researchers carried out the testing at the Macro Lab, TU Delft, using a force controller to examine the static and dynamic behavior of a synthetic mooring cable under various configurations. The experiments are performed at a constant room temperature of the laboratory, which is around 23^oC. The hydraulic jack operated with one fixed and one moving crosshead. Researchers continuously logged several output parameters, including applied force, time, and total elon-

gation, which represented the movement of the hydraulic ram in the testing machine, and tested the sample under dry conditions. Fig.1 (a,b) illustrates the sample rope and test setup, which includes the total length of the samples, the measuring length and the configuration of the loading pins. The initial (unspliced) length of the sample was 2.6 m. In the results analysis, we have calculated the elongation of the sample as the ratio of elongation relative to the total length. A diagram of the jacking machine used in the experiments is shown in Figure 2.
The experimental setup, illustrated in Figure 2, included additional instrumentation such as digital cameras to monitor strain and deformation in the unspliced segment.

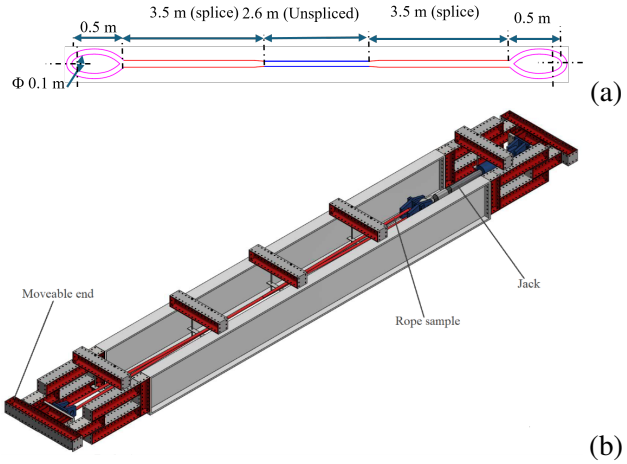

Fig. 1 (a) sample of rope, (b) Isometric view of framed set-up for rope test

Measurement and Data Acquisition

Instrumentation in the experimental setup provided measurements of force, displacement, and strain. Digital cameras tracked markers placed on the ropes, see picture in Figure 2, allowing for a detailed analysis of deformation. The strain was directly measured during the tests. However, due to an incomplete strain dataset, in this work we report the strain calculated from the total displacement at the jack. Periodic temperature monitoring ensured that environmental factors were accounted for, although temperature control was not a primary focus of the study.

Testing Procedures

The experimental program consisted of three primary tests designed to investigate the ropes' mechanical performance:

- **Bedding-In Tests:** Cyclic loading ranging between 10% and 30% of Maximum Breaking Load (MBL) to stabilise the mechanical properties of the rope.
- **Quasi-Static Stiffness Tests:** Gradual loading and unloading cycles to measure the stiffness of the ropes.
- **Dynamic Stiffness Tests:** Cyclic loading at various amplitudes and frequencies to evaluate the ropes' frequency-dependent behaviour and hysteresis.

In what follows we describe in detail the procedure used in the quasi-static stiffness test and dynamic stiffness test.

Quasi-Static Stiffness (QS)

Quasi-static stiffness tests measured the ropes' response to gradual loading and unloading cycle. The tension was incrementally increased in steps of 20 kN from 35 kN (3.5% MBL) until a maximum of 390 kN

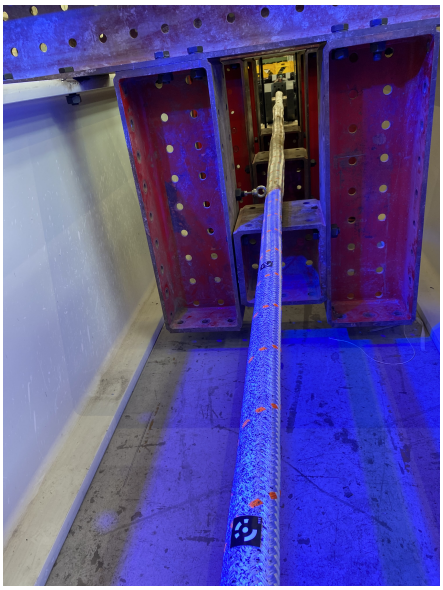

Fig. 2 Picture of the experimental setup with a rope with printed trackers for the Digital Image Correlation system.

(39% MBL). Each step was held for a period of 100 seconds, allowing for relaxation and creep. This protocol followed recommendations by Casey et al. (Casey et al. 2000) and Lechat (Lechat 2007), ensuring accurate stiffness evaluation. In Figure 3 we depict the loading protocol followed for the quasi-static stiffness characterization test.

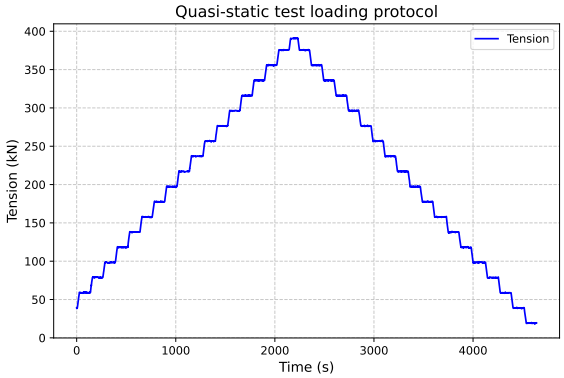

Fig. 3 Quasi-Static Stiffness loading protocol.

Dynamic Stiffness (DS)

Dynamic stiffness tests evaluated the rope's frequency-dependent behaviour and hysteresis. Cyclic loading was applied around five different mean loads: 5%MBL, 10%MBL, 15%MBL, 20%MBL and 225kN (mean load limmited by the jack capacity). We consider four different amplitudes for each mean load (ML): 20%ML, 40%ML, 60%ML and 80%ML. For the last mean load the amplitude has been limited to a maximum total tension of 390kN. For each amplitude we test with three different periods 100s, 15s and 8s. Note that for large amplitudes some of the fast cycles are not carried out due to limitations of the jack speed. Each test included 50, following a similar protocol as proposed in (Thuilliez et al. 2023). This test simulated real-world operational conditions, providing insights into the dynamic performance of the rope. In Fig-

ure 4 we depict the loading protocol followed for the dynamic stiffness characterization test.

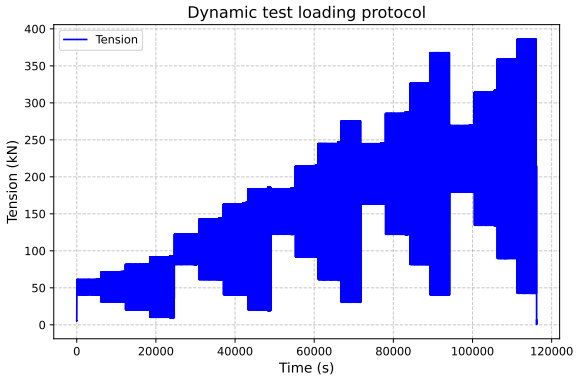

Fig. 4 Dynamic Stiffness loading protocol.

Results

Quasi-Static Response

The results of the quasi-static test for the polyester rope are illustrated in Figures 5 and 6. In these figures we can observe the viscoelastic nature of the response of the curve, following a different path in the loading and unliading branches. We also observe that the loading path in a quasi-static setting follows a curve that has low dependency on the tension level.

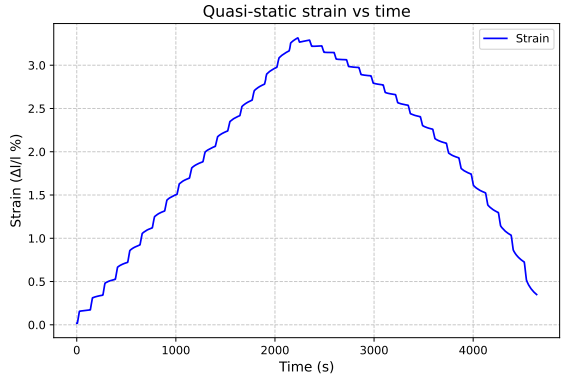

Fig. 5 Strain vs time for the quasi-static stiffness test.

Dynamic Response

In Figure 9 we depict the strain evolution over time for the dynamic loading protocol shown in Figure 4. In this figure we observe the nonlinear dependence of the rope response with respect to mean load, amplitude and loading frequency.

In order to distinguish better the dynamic response of the structure, in Figure 8 we show the evolution of the addimensional dynamic stiffness K_{rd}.

$$K_{rd} = \frac{EA}{MBL}. \tag{1}$$

The axial stiffness, EA, has been computed for each cycle by using extreme points of the strain-tension cycle curve. Each point in Figure 8

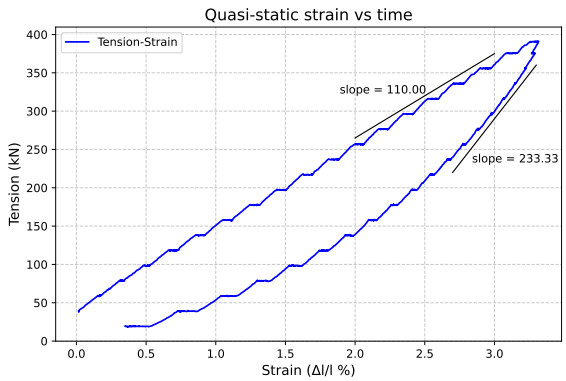

Fig. 6 Tension vs strain for the quasi-static stiffness test.

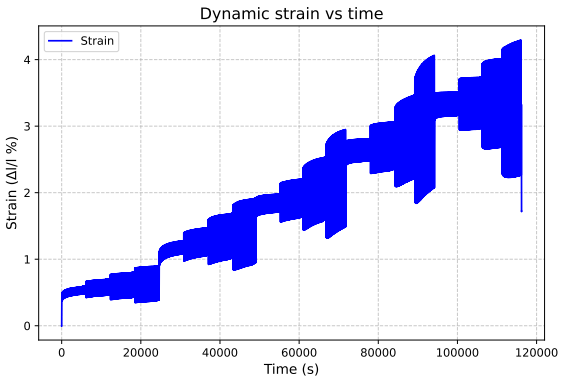

Fig. 7 Strain vs time for the dynamic stiffness test.

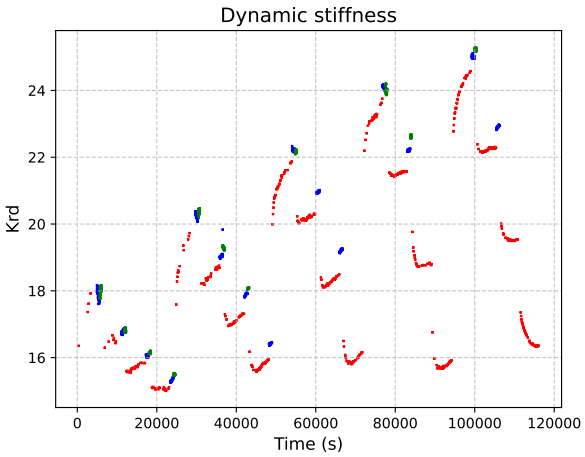

Fig. 8 K_{rd} value for the dynamic stiffness test.

represents a cycle. Note that the points are colored to distinguish the frequency of the cycle: period of 100s in red, 15s in blue and 8s in green. In this figure we can observe the different trends of the dynamic stiffness. When mean load is increased, the dynamic stiffness is increased. When amplitude is increased, the dynamic stiffness decreases. Finally, when frequency is increased, the dynamic stiffness also increases.

Viscoelastic Material Model

Model description

The viscoelastic behaviour of synthetic mooring lines under cyclic and sustained loading is modelled using Schapery's nonlinear viscoelastic framework (Schapery 1969a,b). This approach, widely adopted for time-dependent materials, effectively captures the delayed strain response and internal energy dissipation, which is critical for understanding the dynamic behaviour of mooring lines.

The viscoelastic strain ε_v is expressed as a combination of instantaneous, transient, and load-rate-dependent responses:

$$\varepsilon_v = g_0 D_0 \sigma(t) + g_1 \int_0^t \Delta D\left(\psi(t) - \psi(\tau)\right) \frac{d(g_2\sigma)}{dt}\, d\tau \tag{2}$$

Here, g_0, g_1, and g_2 are material compliance parameters incorporated directly into the model to account for instantaneous, transient, and load-rate-dependent compliance, respectively. The applied stress $\sigma(t)$ acts as a function of time, with D_0 representing the instantaneous compliance, which is the inverse of the initial modulus.

The transient compliance ΔD is expanded as:

$$\Delta D(\psi) = \sum_{n=1}^{N} D_n \left[1 - e^{-\lambda_n \psi}\right] \tag{3}$$

Here, D_n and λ_n denote the n^{th}-order coefficients and retardation times. The reduced time ψ, which scales time effects in the model, incorporates environmental and loading conditions as:

$$\psi = \int_0^t \frac{ds}{a_T a_\sigma a_\varepsilon} \tag{4}$$

In this expression, a_T, a_σ, and a_ε represent scaling factors for temperature, stress, strain, and moisture effects.

Model Calibration from Experiments

The viscoelastic parameters g_0, g_1, and g_2 were calibrated using dynamic test data. The experimental data provided a basis for determining the coefficients D_n, λ_n, and D_0. A linear segment of the stress-strain curve defined the initial modulus E_0, with compliance $D_0 = 1/E_0$. The transient compliance coefficients D_n were optimised using iterative methods to minimise the error function:

$$h(\varepsilon) = \varepsilon - \varepsilon_v \tag{5}$$

where ε is the experimental strain, and ε_v is the predicted strain from the viscoelastic model.

Numerical Solution of the Viscoelastic Model

The viscoelastic response is computed efficiently using a hereditary integral approach, allowing incremental strain updates across time steps by reusing previous calculations. The hereditary integral, represented by $q_n(t - \Delta t)$, is updated as follows:

$$q_n(t) = e^{-\lambda_n \Delta\psi} q_n(t - \Delta t) + \left(1 - e^{-\lambda_n \Delta\psi}\right) \frac{g_2\sigma(t) - g_2(t - \Delta t)\sigma(t - \Delta t)}{\lambda_n \Delta\psi} \tag{6}$$

The derivatives of the viscoelastic strain ε_v with respect to stress are computed as:

$$\frac{d\varepsilon_v}{d\sigma} = \frac{d\Psi}{d\sigma} + \frac{d\Phi}{d\sigma} \tag{7}$$

where Ψ and Φ are given by:

$$\begin{aligned}\Psi(\sigma) = {} & g_0(\sigma) D_0 + g_1(\sigma) g_2(\sigma) \sum_{n=1}^{N} D_n \left(1 - e^{-\lambda_n \Delta\psi}\right) \\ & - g_1(\sigma) g_2(\sigma) \sum_{n=1}^{N} D_n \frac{1 - e^{-\lambda_n \Delta\psi}}{\lambda_n \Delta\psi}\end{aligned} \tag{8}$$

$$\begin{aligned}\Phi(\sigma) = {} & g_1(\sigma) \sum_{n=1}^{N} D_n \Big(e^{-\lambda_n \Delta\psi} q_n(t - \Delta t) \\ & - g_2(\sigma)(t - \Delta t) \left[1 - e^{-\lambda_n \Delta\psi}\right] \frac{\sigma(t - \Delta t)}{\lambda_n \Delta\psi} \Big)\end{aligned} \tag{9}$$

An iterative optimization adjusts σ to satisfy:

$$h(\varepsilon) = \varepsilon - \varepsilon_v \tag{10}$$

The objective is to minimise $h(\varepsilon)$ toward zero, signaling convergence.

Numerical Implementation and Results

The numerical model employed a hereditary integral approach for efficient computation, updating strain incrementally over time. Parameters D_0, D_n, g_0, g_1, and g_2 were calibrated from the cyclic loading tests. Using the `Optim.jl` package in Julia, Particle Swarm Optimization refined the parameters to align the modeled responses with experimental data.

Applying the dynamic parameters to cyclic conditions allowed the model to capture the viscoelastic strain evolution under repetitive loading and unloading cycles. The results demonstrate reasonable agreement between the modeled and experimental data, with deviations typically under 5%.

Results

The viscoelastic model, incorporating g_0, g_1, and g_2 parameters, demonstrated robust performance in simulating the stress-strain and time-dependent behaviour of synthetic mooring lines under dynamic (DS) loading conditions. The model accurately represented cyclic strain evolution and energy dissipation using parameters calibrated from QS tests. The inclusion of transient (g_1) and load-rate-dependent (g_2) compliance allowed the model to align closely with experimental data, capturing internal energy dissipation through hysteresis loops and replicating the viscoelastic response under sustained and repetitive loading.

In Table 1 we report the model parameters fitted with the dynamic test protocol. Here, we used $N = 8$ with $\lambda_n = \{1.0e^{-1}, 1.0e^{-2}, 1.0e^{-3}, 1.0e^{-4}, 1.0e^{-5}, 1.0e^{-6}, 1.0e^{-7}, 1.0e^{-8}\}$. The model parameters g_0, g_1, and g_2 are assumed to have a cubic dependence with respect to the stress.

Table 1 Viscoelastic parameters employed in quasi-static test for Rope 1.

Viscoelastic Parameter		
n	λ_n (s^{-1})	D_n (10^{-10} **Pa**$^{-1}$)
1	10^{-1}	1.0
2	10^{-2}	1.5
3	10^{-3}	1.0
4	10^{-4}	1.5
5	10^{-5}	20.0
6	10^{-6}	1.0
7	10^{-7}	1.0
8	10^{-8}	100.0
D_0		1.97
$g_0 = 0.55 - 1.0e^{-10}\,\sigma - 3.0e^{-18}\,\sigma^2 + 1.0e^{-26}\,\sigma^3$		
$g_1 = 0.1 + 6.6e^{-11}\,\sigma + 4.2e^{-19}\,\sigma^2 - 2.7e^{-27}\,\sigma^3$		
$g_2 = 1.7 - 8.8e^{-9}\,\sigma + 4.4e^{-17}\,\sigma^2 + 5.0e^{-28}\,\sigma^3$		

In Figure 9 we depict the viscoelastic model prediction, overlapped with the experimental data. It can be observed that the model is able to reproduce the overall dynamic response of the rope. We also see that Schapery's viscoelastic model behaves well for various mean loads, cycle amplitudes and loading frequencies. For the maximum amplitude cycles the model cannot capture accurately the dynamic effects.

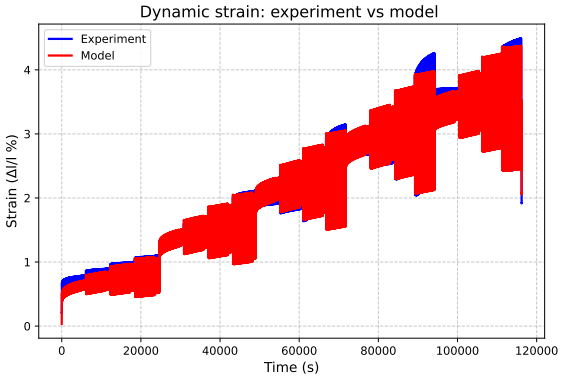

Fig. 9 Strain vs time for the dynamic stiffness test. The viscoelastic model is red, and the experimental data is blue.

CONCLUSIONS

The study successfully applied and validated a viscoelastic model capturing synthetic mooring lines' nonlinear, time-dependent, and frequency-dependent behaviour under dynamic loading conditions. The model demonstrated excellent alignment with observed mechanical responses by integrating experimental data with numerical simulations.

Note that the results from this model are applicable to the conditions and rope characteristics tested in the experiments, scaling effects should be further studied. Future work will extend the model to account for additional environmental factors such as temperature and moisture variations, further enhancing its predictive capability and reliability in diverse offshore applications. Furthermore, in follow-up works this model will be implemented in a finite element model for the dynamic assessment of synthetic mooring lines.

ACKNOWLEDGMENTS

This publication is part of the project MERGANSER with file number DEI122010 of the programme DEI+ from the Netherlands Enterprise Agency (RVO).

REFERENCES

Bain, Cédric et al. . "Influence of bedding-in on the tensile performance of HMPE fiber ropes". In: *Ocean Engineering* 203, p. 107144. ISSN: 0029-8018. DOI: 10.1016/J.OCEANENG.2020.107144.

Casey, N.F. et al. . "Short- and Long-Term Property Behaviour of Polyester Rope". In: *Proceedings of the Offshore Technology Conference*. OTC 12177. Houston, Texas, USA, pp. 1–12.

Chailleux, E. and P. Davies. "A Non-Linear Viscoelastic Viscoplastic Model for the Behaviour of Polyester Fibres". In: *Mechanics of Time-Dependent Materials* 9, pp. 147–160. DOI: 10.1007/s11043-005-6034-y.

Chevillotte, Yoan et al.. "Fatigue of improved polyamide mooring ropes for floating wind turbines". In: *Ocean Engineering* 199, p. 107011. ISSN: 00298018. DOI: 10.1016/j.oceaneng.2020.107011.

Davies, P. et al.. "Mechanical behaviour of HMPE and aramid fibre ropes for deep sea handling operations". In: *Ocean Engineering* 38.17–18, pp. 2208–2214. DOI: 10.1016/j.oceaneng.2011.10.010. URL: https://doi.org/10.1016/j.oceaneng.2011.10.010.

Huang, Wei et al.. "Modeling nonlinear time-dependent behaviors of synthetic fiber ropes under cyclic loading". In: *Ocean Engineering* 109, pp. 207–216. ISSN: 0029-8018. DOI: 10.1016/j.oceaneng.2015.09.009. URL: https://www.sciencedirect.com/science/article/pii/S0029801815004746.

Lechat, Céline. "Comportement mécanique de fibres et d'assemblages de fibres en polyester pour câbles d'amarrage de plates-formes offshore". Theses. École Nationale Supérieure des Mines de Paris. URL: https://pastel.hal.science/tel-00280511.

Lian, Yushun et al. . "An experimental investigation on the bedding-in behavior of synthetic fiber ropes". In: *Ocean Engineering* 160, pp. 368–381. ISSN: 0029-8018. DOI: 10.1016/J.OCEANENG.2018.04.071.

Nguyen, T. and K. Thiagarajan. "Nonlinear viscoelastic modeling of synthetic mooring lines". In: *Ocean Engineering* 242, p. 110040. DOI: 10.1016/j.oceaneng.2021.110040.

Schapery, R.A.. "On the characterization of nonlinear viscoelastic materials". In: *Journal of Composite Materials* 3.3, pp. 480–502. DOI: 10.1177/002199836900300305.

— . "On the characterization of nonlinear viscoelastic materials". In: *Polymer Engineering & Science* 9.4, pp. 295–310. DOI: 10.1002/pen.760090410. URL: https://4spepublications.onlinelibrary.wiley.com/doi/abs/10.1002/pen.760090410.

Thuilliez, Hugo et al.. "Characterization and modelling of the dynamic stiffness of nylon mooring rope for floating wind turbines". In: *Ocean Engineering* 287, p. 115866.

Weller, S.D. et al.. "Synthetic mooring ropes for marine renewable energy applications". In: *Renewable Energy* 83, pp. 1268–1278. ISSN: 09601481. DOI: 10.1016/j.renene.2015.03.058.

Weller, Sam et al. . "Synthetic rope responses in the context of load history: Operational performance". In: *Ocean Engineering* 83, pp. 111–124. DOI: 10.1016/j.oceaneng.2014.03.010.